

Transitions of I- and II-order in magnetic field for superconducting cylinder from self-consistent solution of Ginzburg–Landau equations

G.F. Zharkov

P.N. Lebedev Physics Institute, Russian Academy of Sciences, Moscow, 117924, Russia

(October 2, 2000)

Basing on self-consistent solution of non-linear GL-equations, the phase boundary is found, which divides the regions of I- and II-order phase transitions of a superconducting cylinder in magnetic field to normal state. This boundary is a complicated function of the parameters (m, R, \varkappa) (m is the vorticity, R is the cylinder radius, \varkappa is the GL-parameter), which does not coincide with the simple phase boundary $\varkappa = 1/\sqrt{2}$, dividing the regions of I- and II-order phase transitions in infinite (open) superconducting systems.

I. INTRODUCTION

The GL-theory is widely used for studying the general properties of the superconducting state. This theory leads to two coupled non-linear equations for the order parameter ψ and the magnetic field vector-potential \mathbf{A} , which are usually solved using various simplifying assumptions. In a number of papers [2–8] the particular case was considered of a long superconducting cylinder of radius R , placed in the axial magnetic field H . In this case the 3-dimensional GL-equations reduce to one-dimensional form, which enables one to find numerically the exact self-consistent solutions. In such way it is possible to study specific non-linear effects, as well as the role of the sample boundary. For instance, it was shown in [6,7], that one-dimensional solution for the order parameter ψ (with fixed vorticity m and varying H) may change its form either gradually (in one interval of parameters (R, \varkappa) , \varkappa is the GL-parameter), or abruptly (in the other interval of (R, \varkappa)), undergoing I-order jump transformation. Such jump transformations, in principle, may be observable, because they are accompanied by jumps of the magnetisation, $M(H)$.

In the present paper the phase boundary is found, which divides the region of parameters (R, \varkappa) , where the superconducting solution (of fixed m) ends up (in the increasing external field) by I-order jump to normal state ($\psi \equiv 0$), from the region (R, \varkappa) , where the solution vanishes gradually, by II-order phase transition. This phase boundary is a complicated function of R and \varkappa , different from the simple boundary $\varkappa = 1/\sqrt{2}$, which divides the I- and II-order phase transitions in infinite (open) superconductors [9]. Other topics are also touched on (such as metastability, the paramagnetic Meissner effect, the pinning of vortices to the sample boundary, the linearized equation approximation, etc.).

In Sec. II the problem is formulated and the basic GL-equations, used in calculations, are written. Sec. II contains the numerical results, alongside with necessary

comments. In Sec. IV the results are summarized and discussed.

II. EQUATIONS

Below the case is considered of a long superconducting cylinder of radius R , in the external magnetic field $H \geq 0$, which is parallel to the cylinder element. In the cylindrical co-ordinates the system of GL-equations may be written in dimensionless form [6]

$$\frac{d^2 U}{d\rho^2} - \frac{1}{\rho} \frac{dU}{d\rho} - \psi^2 U = 0, \quad (1)$$

$$\frac{d^2 \psi}{d\rho^2} + \frac{1}{\rho} \frac{d\psi}{d\rho} + \varkappa^2 (\psi - \psi^3) - \frac{U^2}{\rho^2} \psi = 0. \quad (2)$$

Here $U(\rho)$ is the dimensionless field potential; $b(\rho)$ is the dimensionless magnetic field; $\psi(\rho)$ is the normalized order parameter; $\rho = r/\lambda$, λ is the field penetration length; $\lambda = \varkappa \xi$, where ξ is the coherence length, \varkappa is the GL-parameter. The dimensioned potential A , field B and current j_s are related to the corresponding dimensionless quantities by the formulae [6]:

$$A = \frac{\phi_0}{2\pi\lambda} \frac{U + m}{\rho}, \quad B = \frac{\phi_0}{2\pi\lambda^2} b, \quad b = \frac{1}{\rho} \frac{dU}{d\rho},$$

$$j(\rho) = j_s / \frac{c\phi_0}{8\pi^2\lambda^3} = -\psi^2 \frac{U}{\rho}, \quad \rho = \frac{r}{\lambda}. \quad (3)$$

(The field B in (3) is normalized by $H_\lambda = \phi_0/(2\pi\lambda^2)$, with $b = B/H_\lambda$; instead of H_λ one can normalize by $H_\xi = \phi_0/(2\pi\xi^2)$, or by $H_\varkappa = \phi_0/(2\pi\xi\lambda) = H_\xi/\varkappa$. The coefficients in (1), (2) would change accordingly.) The vorticity m in (3) specifies how many flux quanta are associated with the vortex, centered at the cylinder axis (the so-called giant-vortex state).

The boundary conditions to Eq. (1) are [7]:

$$U|_{\rho=0} = -m, \quad \left. \frac{dU}{d\rho} \right|_{\rho=\rho_1} = h_\lambda. \quad (4)$$

where $\rho_1 = R/\lambda$, $h_\lambda = H/H_\lambda$.

The boundary conditions to Eq. (2) are [7]:

$$\begin{aligned} \left. \frac{d\psi}{d\rho} \right|_{\rho=0} = 0, \quad \left. \frac{d\psi}{d\rho} \right|_{\rho=\rho_1} = 0 \quad (m=0), \\ \psi|_{\rho=0} = 0, \quad \left. \frac{d\psi}{d\rho} \right|_{\rho=\rho_1} = 0 \quad (m>0). \end{aligned} \quad (5)$$

The magnetic moment (or, magnetisation) of the cylinder, related to the unity volume, may be written in a form

$$\frac{M}{V} = \frac{1}{V} \int \frac{B-H}{4\pi} dv = \frac{B_{av} - H}{4\pi},$$

$$B_{av} = \frac{1}{V} \int B(\mathbf{r}) dv = \frac{1}{S} \Phi_1,$$

where B_{av} is the mean field value inside the superconductor, Φ_1 is the total magnetic flux, confined in the cylinder. In the normalization (3), denoting $\bar{b} = B_{av}/H_\lambda$, $h_\lambda = H/H_\lambda$, $M_\lambda = M/H_\lambda$, one finds

$$\begin{aligned} 4\pi M_\lambda = \bar{b} - h_\lambda, \quad \bar{b} = \frac{2}{\rho_1^2} (U_1 + m), \quad (6) \\ \phi_1 = \frac{\Phi_1}{\phi_0} = U_1 + m, \quad U_1 = U(\rho_1), \quad \rho_1 = \frac{R}{\lambda}. \end{aligned}$$

Accordingly, the normalized Gibbs free energy of the system may be written as [7]

$$\begin{aligned} \Delta g = \Delta G / \left(\frac{H_{cm}^2}{8\pi} V \right) = g_0 - \frac{8\pi M_\lambda}{\varkappa^2} h_\lambda + \frac{4m}{\varkappa^2} \frac{b(0) - h_\lambda}{\rho_1^2}, \\ g_0 = \frac{2}{\rho_1^2} \int_0^{\rho_1} \rho d\rho \left[\psi^4 - 2\psi^2 + \frac{1}{\varkappa^2} \left(\frac{d\psi}{d\rho} \right)^2 \right]. \end{aligned} \quad (7)$$

Here $\Delta G = G_s - G_n$ is the difference of free energies in superconducting and normal states; $b(0) = B(0)/H_\lambda$, $B(0)$ is the magnetic field at the cylinder axis; $H_{cm} = \phi_0/(2\pi\sqrt{2}\lambda\xi)$ is thermodynamical critical field of massive superconductor; g_0 is the condensation energy with account for the order parameter gradient. The expressions (6), (7) may be used for calculating the corresponding quantities. [Instead of ρ_1 the notation $R_\lambda = R/\lambda \equiv \rho_1$ will be used below.]

III. NUMERICAL RESULTS

The solutions of Eqs. (1)–(5) depend on the space coordinate ρ and several parameters, for instance, $\psi(\rho) =$

$\psi(m, R_\lambda, \varkappa, h_\lambda; \rho)$ (analogously for the potential $U(\rho)$ and the field $b(\rho)$). Let the vorticity m be fixed ($m = 0, 1, 2, \dots$) and consider at first the case $m = 0$ (the vortex-free Meissner state). Consider the plane of parameters (R_λ, \varkappa) (see Fig. 1(a)). In every point of this plane there exists a set of solutions of Eqs. (1)–(5), which depend parametrically on the external field h_λ . (Several points, laying along the line $R_\lambda = 4$ are numerated as 1-6.) One may envisage a peep-hole, peared in every point (R_λ, \varkappa) , which allows to see the content of the corresponding sub-volume. The set of solutions $\psi(h_\lambda; \rho)$ is unique for each sub-volume and may be characterised, for instance, by the field dependence of the maximal value of the order parameter $\psi_{max}(h_\lambda)$, or by the form of the magnetisation curve $M_\lambda(h_\lambda)$ (6). The examples of such dependencies in different points of the plane (R_λ, \varkappa) are given in Figs. 1(b, c) (only the case $h_\lambda \geq 0$ is considered; some illustrations for the case $h_\lambda < 0$, as well as the corresponding co-ordinate dependencies, may be found in [6,7]).

It is clear from Fig. 1(b), that the characteristic behavior $\psi_{max}(h_\lambda)$ depends essentially on the value of \varkappa . For small \varkappa , the value $\psi_{max}(h_\lambda)$ terminates (the curves 1-4) by jump at some point $h_\lambda = h_s$, where (if h_λ is increased) the I-order phase transition to normal state ($\psi(\rho) \equiv 0$) occurs. The region, where the superconducting solutions terminate by I-order phase transition, is marked in Fig. 1(a) as s_I .

For larger \varkappa (the curves 5,6) there is also a jump in $\psi_{max}(h_\lambda)$ at some point $h_\lambda = h_s$, but with a "tail" appearing on the curve. If the field h_λ increases, the superconducting solutions 5,6 vanish gradually at the point h_c , by II-order phase transition to normal state. The region, where the superconducting solutions terminate by II-order phase transition, is marked in Fig. 1(a) as s_{II} . [The appearance of the tail on the magnetisation curve means the transition of the solution to the edge-suppressed form, see [7] for details.]

It is evident, that for small radius cylinder ($R_\lambda < 1.69$) the superconducting solution terminates by II-order phase transition, even in type-1 (i.e. small \varkappa) superconductors [10]. The transformation of the solutions with diminishing radius R_λ is illustrated in Fig. 2 for $\varkappa = 0.7$.

Note, that if the line $\varkappa = 1$ in Fig. 1(a) is followed from large to small R_λ , the superconducting states, which lay along this line, display at first the II-order phase transition in magnetic field (for larger R_λ), then the I-order (for intermediate R_λ), and again the II-order (for smaller R_λ). Only, if $\varkappa > 1.05$, all the solutions display II-order behavior.

Notice also, that the state $m = 0$ is totally diamagnetic ($-4\pi M_\lambda > 0$).

Because in every point of s_{II} -region the order parameter vanishes by II-order phase transition ($\psi_{max} \rightarrow 0$, see Fig. 1(b)), the superconducting phase boundary in magnetic field, h_c , may be found analytically, by lineariz-

ing the system (1), (2) (with account, that $\psi \ll 1$ and $b \approx h_\lambda$), and passing to single linear equation for the order parameter [11], whose solution may be expressed in terms of the Kummer functions (see also [3,4,5,12]). However, inside s_I -region (where the solution terminates by jump from a finite value ψ_{max} to zero) the phase boundary h_s (i.e. the highest field h_λ still compatible with the superconductivity) can not be found by solving the linearized equation, but full system (1)–(5) is needed.

The analogous investigation can be carried out in the case $m = 1$ (see Fig. 3), with a single vortex on the cylinder axis.

In Fig. 3(a) are shown: the region s_I , where the superconducting state terminates (if the field is increased) by I-order jump to the normal state, having finite value ψ_{max} at the transition point; the region s_{II} , where the superconductivity vanishes by II-order phase transition; the curve s_{I-II} , which represents the boundary between I- and II-order phase transitions.

The behavior of the order parameter $\psi_{max}(h_\lambda)$ and of the magnetisation $M_\lambda(h_\lambda)$ in different points of the plane (R_λ, \varkappa) are shown in Figs. 3(b, c) (and in Fig. 4). For small \varkappa (the curves 1,2) the solutions terminate by I-order jump. When the line s_{I-II} is crossed, the tail appears on the curves 3,4, which widens, if R_λ and \varkappa increase. If R_λ diminishes (Fig. 4), the magnitude of the jump in ψ_{max} also diminishes, and the solutions terminate (if the field is increased) by II-order phase transition to normal state.

On the curve C_{ns} (Fig. 3(a)) the value $\psi_{max} = 0$. The letter n denotes the normal metal region ($\psi \equiv 0$); here the superconducting state ($m = 1$) is impossible. [In this region the radius R_λ is too small, and the vortex own field is too strong to be confined within the mesoscopic sample.] It is evident, that when the radius R_λ diminishes (but \varkappa is fixed) the transition from s - to n -state always is II-order phase transition, however the width of the region between the curves s_{I-II} and C_{ns} (where II-order transition exists) gets very small for small \varkappa . The curve C_{ns} may be well approximated by the dependence $R_\lambda \sim a/\varkappa$ (or $R_\xi = \varkappa R_\lambda = a$), with $a = 1.34$.

Notice, that in any point of s -region in Fig. 3(a) the magnetisation function $M_\lambda(h_\lambda)$ (Fig. 3(c)) has two parts: the paramagnetic ($M_\lambda > 0$) and diamagnetic ($M_\lambda < 0$). This is because the superconducting current has two components, $j_s = j_p + j_d$. One of these currents (j_p) screens the own field of the vortex ($m = 1$) and flows around the vortex axis in counter-clockwise direction (the paramagnetic current). The second current (j_d) screens out the external field h_λ and flows near the cylinder surface in clock-wise direction (the diamagnetic current). Depending on which of these currents prevail, the magnetisation (or, equivalently, the magnetic moment $M_\lambda = (1/2c) \int [\mathbf{j}_s \mathbf{r}] dv$) can change sign, as function of h_λ (see [8] for details). Recall, that in the vortex-free state ($m = 0$) there exists only diamagnetic current, i.e.

$M_\lambda < 0$, see Fig. 1(c). In presence of the vortex ($m = 1$), but in absence of the external field ($h_\lambda = 0$), the screening current and the magnetic moment correspond to the paramagnetic state. This state is metastable, because the vortex-free state possesses smaller free-energy, than the state $m = 1$ [2–8].

The curve P_0 in Fig. 3(a) corresponds to the minimal radius R_λ , when the paramagnetic vortex state ($m = 1$) can still exist inside the homogenous cylinder in absence of the field ($h_\lambda = 0$). [The metastable vortex is held inside by the pinning to the cylinder boundary.] In those points (R_λ, \varkappa) , which lay below the curve P_0 , to hold the vortex inside the cylinder it is necessary to impose a finite external field, $h_\lambda > 0$. (This corresponds to the field stimulated and re-entrant superconductivity [2–8].) Notice, that if the cylinder radius R and the parameter \varkappa are fixed, to cross the paramagnetic pinning boundary (P_0) it is sufficient to vary only the sample temperature, because $R_\lambda = R/\lambda(T)$.

The presence of a smooth tail in the function $\psi_{max}(h_\lambda)$ [Figs. 3(b) and 4(a)] allows (as in the case $m = 0$) to use the linear approximation ($\psi \ll 1$) for finding the upper boundary of the superconducting state, h_c . In the region of I-order jumps [s_I in Fig. 3(a)], where the function $\psi(\rho)$ is not small, the linear approach fails and more rigorous analysis, based on full system of non-linear equations (1)–(5), is necessary. [The boundaries $s_{I-II}(\varkappa)$ and $C_{ns}(\varkappa)$ themselves can not be found from the linear equation, because the latter does not depend on \varkappa [11]. The comparison of the results of the rigorous and linear analysis will be reported elsewhere.]

Similarly, one can consider the higher giant-vortex states ($m > 1$, see Fig. 5 for $m = 2$). Here also exist the boundaries of I- and II-order phase transitions, the jumps on the magnetisation curves, the paramagnetic and diamagnetic currents, and other peculiarities, which are analogous to those presented in Figs. 1–4.

IV. CONCLUSION AND DISCUSSION

Basing on self-consistent solution of non-linear system of GL-equations, the boundary, s_{I-II} , is found, which separates the regions, where the superconducting state of the cylinder is destroyed by the external magnetic field either by I-order jump (the region s_I), or gradually, by II-order phase transition (the region s_{II}). This boundary is a complicated function of the parameters $(m, R_\lambda, \varkappa)$ [see Figs. 1(a), 3(a), 5].

Note, that in the case of an infinite (open) superconductor the phase boundary between I- and II-order transitions lays at the value $\varkappa = 1/\sqrt{2}$ [9]. (At this value the surface energy at the interface of superconducting and normal metals vanishes, and the magnetisation $M(H)$ acquires a smooth tail [9].) However, the case of infinite superconductor is degenerated, in the sense that the

total number of vortices in the open system can not be defined. Due to this degeneration there are many solutions of the system (1), (2) with different m , and it is possible to consider the superconducting state as a linear combination of states with different vorticities m [9]. In the bounded system this degeneracy is removed, and it is necessary to consider the states of fixed vorticity m (the quantum number m is now a topological invariant). [It is easy to prove that self-consistent solution of Eqs. (1)–(5) with $\psi \neq 0$ is unique for every value of h_λ .] The mentioned difference of the s_{I-II} -boundary from the value $\varkappa = 1/\sqrt{2}$ is due to the difference in geometries and to the account of the space-quantization effects, present in the bounded system. [To trace the limiting transition from the bounded to open geometry, it might be necessary to consider the case of flattened elliptical cylinder, which models the geometry of an infinite slab, adopted in [9].]

Mention in conclusion, that the main attention in the present work was paid to the mathematical side of the problem: to describe the s_{I-II} -boundary basing on formal solutions of GL-equations. The important physical question of comparing the Gibbs free energies of various mathematically possible states, and finding the most stable ground state (which the system would occupy in equilibrium), was put aside. (Some illustrations of the Gibbs free energy behavior, found from Eq. (7), are given, for instance, in [6-8].) In justification, it may be reminded, that the physical system may occupy not only the ground state, but also the excited metastable states of higher energy. [In particular, the controversial paramagnetic Meissner effect may be attributed to the metastable vortex states in the mesoscopic system, see [8] for details). The formal solutions of GL-equations describe all possible states, including stable and metastable one, thus the full analysis, based on these equations, may be pertinent to the experiment. However, the case of infinitely long cylinder, considered above, approximates rather poorly the geometry, used in real experiments. In this respect, the superconducting disks, considered in [4,5], are more adequate, though it would be more difficult to obtain rigorous solutions for the bounded 3-dimensional sample. Thus, further analysis of the questions, touched on in the present paper (as well as possible connection with experiment), is necessary.

V. ACKNOWLEDGMENTS

I am grateful to V. L. Ginzburg for the interest in this work and valuable discussions. I thank also F. M. Peeters and J. J. Palacios for sending the reprints of recent papers, where closely connected problems are considered.

- [1] V.L. Ginzburg, L.D. Landau, Zh.Exp.Teor.Fyz., **10**, 1064 (1950).
- [2] H.J. Fink et al., Phys.Rev. **151**, 219, (1996); **168**, 168 (1968); Phys.Rev.B, **20**, 1947 (1979).
- [3] V.V. Moshchalkov, X.G. Qiu, V. Bruyndoncx, Phys.Rev.B**55**, 11 793 (1997).
- [4] J.J. Palacios, Phys.Rev.B **58**, R5948 (1998); Physica B, **256-258**, 610 (1998); Phys.Rev.Lett., **83**, 2409 (1999); **84**, 1796 (2000).
- [5] V.Schweigert, F.Peeters et.al., Phys.Rev.Lett., **79**, 4653 (1997); Supralatt. and Microstruct., **25**, 1195 (1999); Phys.Rev.B**59**, 6039 (1999); Physica C**332**, 266,426,255 (2000); cond-mat/0001110 (2000).
- [6] G.F. Zharkov, V.G. Zharkov, Physica Scripta **57**, 664 (1998); G.F. Zharkov, V.G. Zharkov, A.Yu. Zvetkov, Phys.Rev.B**61**, 12 293 (2000).
- [7] G.F. Zharkov, V.G. Zharkov, A.Yu. Zvetkov, "Self-consistent solutions of G-L-equations and edge-suppressed states in magnetic field", cond-mat/0008217 (2000) (submitted to Phys.Rev.B).
- [8] G.F. Zharkov, "Paramagnetic Meissner effect in superconductors from self-consistent solution of GL-equations", cond-mat/0009043 (2000) (submitted to Phys.Rev.B).
- [9] A.A. Abrikosov, *Fundamentals of the Theory of Metals* (North-Holland, Amsterdam, 1988).
- [10] V.L. Ginzburg, Zh.Exp.Teor.Fyz. **34**, 113 (1958); Soviet Phys.– JETP **7**, 78 (1958).
- [11] D. Saint-James, P. de Gennes, Phys.Lett. **7**, 306 (1963); D. Saint-James, Phys. Lett. **15**, 13 (1965).
- [12] Yu. N. Ovchinnikov, Sov. Phys. JETP, **52**, 755 (1980).

Figures captions

Fig. 1. (a) – The boundary (s_{I-II}) between regions (s_I and s_{II}), where I- or II-order phase transitions to normal state ($\psi \equiv 0$) in magnetic field occur. (b) – The behavior $\psi_{max}(h_\lambda)$ in the points 1-6 ($m = 0$, $R_\lambda = 4$) in Fig. 1(a). In the region s_I the order parameter vanishes by I-order jump. In the region s_{II} the order parameter $\psi_{max}(h_\lambda)$ has a "tail", and vanishes smoothly, by II-order phase transition. (c) – Analogous behavior for magnetisation, $M_\lambda(h_\lambda)$. The peep-holes 1-9 in (a) are pierced in the points: 1 – $\varkappa = 0.2$, 2 – $\varkappa = 0.4$, 3 – $\varkappa = 0.7$, 4 – $\varkappa = 1$, 5 – $\varkappa = 1.05$, 6 – $\varkappa = 1.2$ ($R_\lambda = 4$); 7 – $R_\lambda = 3$, 8 – $R_\lambda = 2$, 9 – $R_\lambda = 1.5$ ($\varkappa = 0.7$).

Fig. 2. The dependencies: (a) – $\psi_{max}(h_\lambda)$ and (b) – $M_\lambda(h_\lambda)$ for $m = 0$, $\varkappa = 0.7$. The numeration of curves correspond to points 3,7-9 in Fig. 1(a).

Fig. 3. Analogous to Fig. 1, but for $m = 1$. The dashed curve C_{ns} in Fig. 3(a) separates the normal (n) and superconducting (s) regions. The curve P_0 marks the points (R_λ, \varkappa), where the metastable vortex state ($m = 1$) may still exist in absence of the field ($h_\lambda = 0$) due to the pinning to the boundary. Below the curve P_0 the vortex state may exist only in presence of finite external field ($h_\lambda > 0$, see the curves 1,2 in Figs. 3(b,c)). (This is an example of the field stimulation effect, or re-entrant superconductivity.) The peep-holes 1-8 in (a) are pierced in the points: 1 – $\varkappa = 0.35$, 2 – $\varkappa = 0.4$, 3 –

$\varkappa = 0.7$, $4 - \varkappa = 1$, $5 - \varkappa = 1.07$, $6 - \varkappa = 1.2$ ($R_\lambda = 4$);
 $7 - R_\lambda = 3$, $8 - R_\lambda = 2.4$ ($\varkappa = 0.7$).

Fig. 4. Analogous to Fig 2, but for $m = 1$. The presence of paramagnetic ($M_\lambda > 0$) and diamagnetic ($M_\lambda < 0$) parts of magnetisation is evident in Fig. 4(b).

Fig. 5. Analogous to Figs. 1(a) and 3(a), but for $m = 2$. The vertical asymptote $\varkappa = 0.94$ is the same for $m = 0, 1, 2$. This is natural, because for large radii ($R_\lambda \gg 1$) the influence of the vortex field is negligible. The bottom of the curve s_{I-II} lays at $R_\lambda = 2.78$ (with $R_\lambda = 2.45$ for $m = 1$, and $R_\lambda = 1.69$ for $m = 0$). The dashed curve C_{ns} is well approximated by the dependence $C_{ns} \approx 1.81/\varkappa$ (the dotted line).

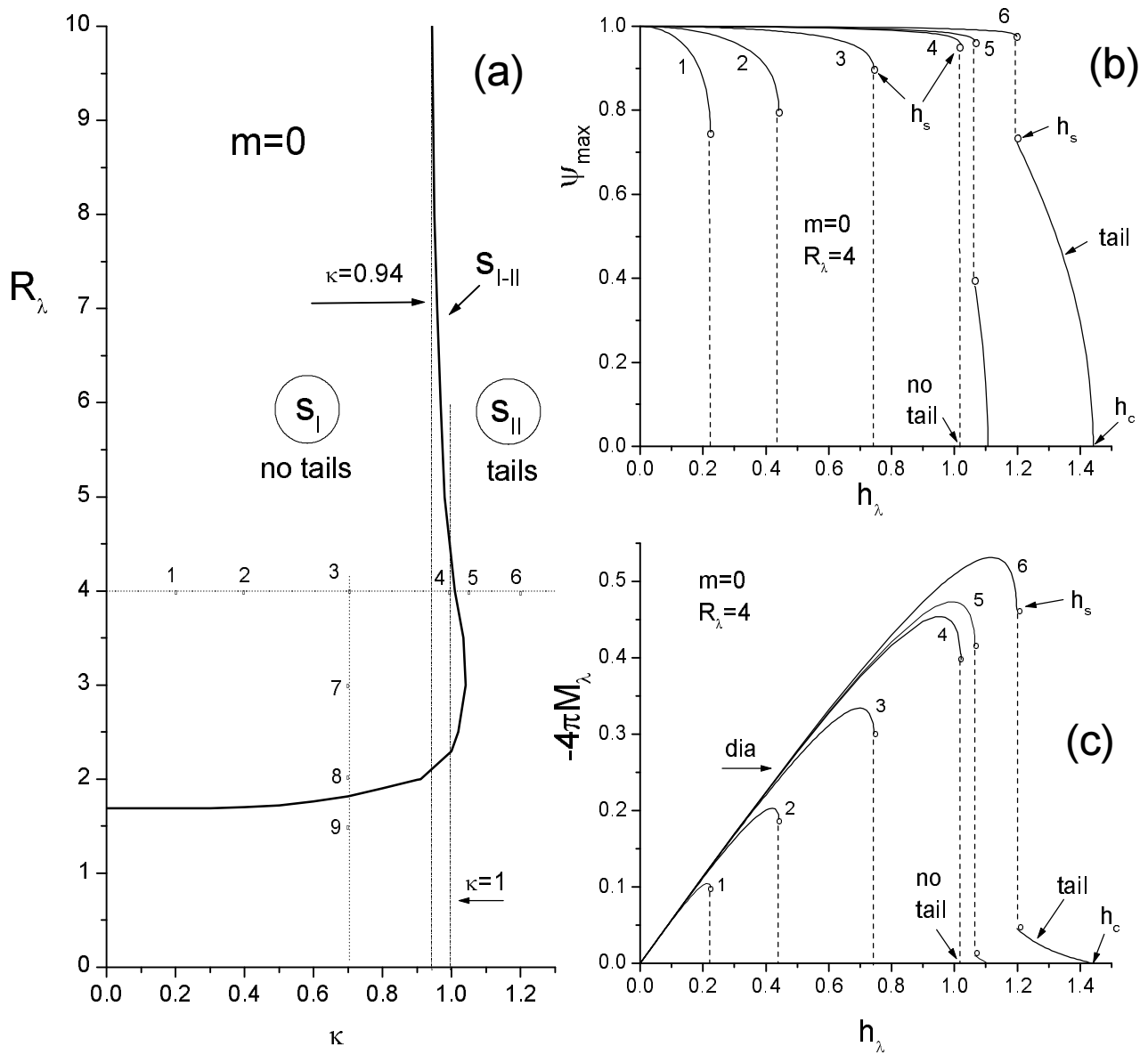


Fig. 1

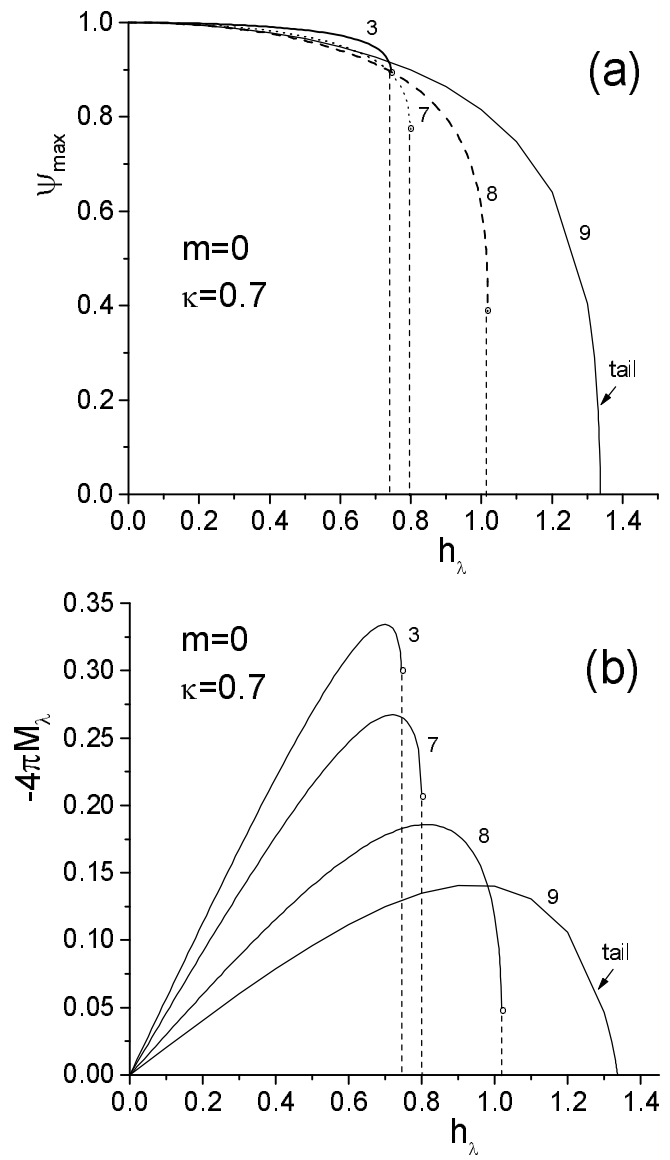


Fig. 2

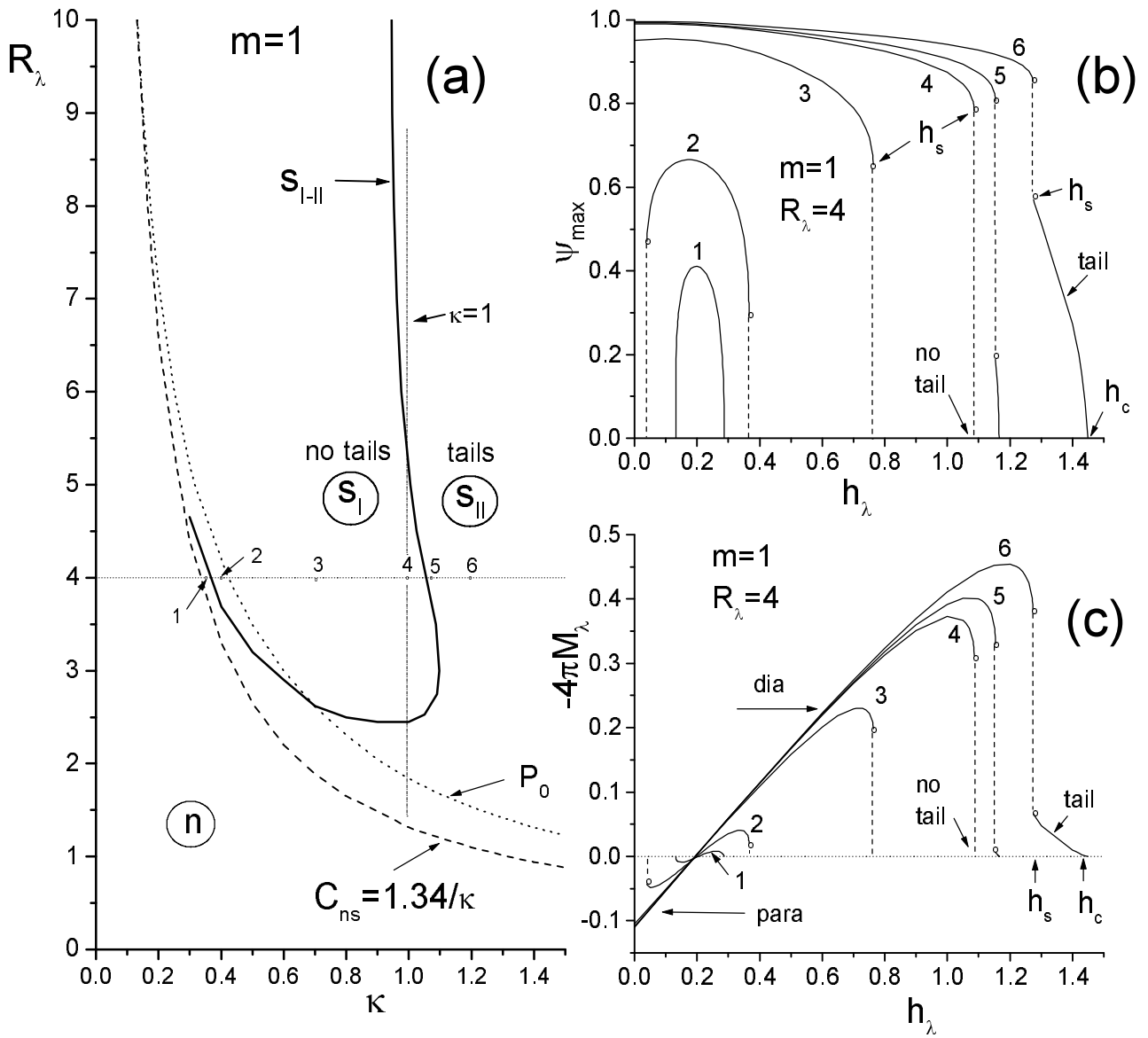


Fig. 3

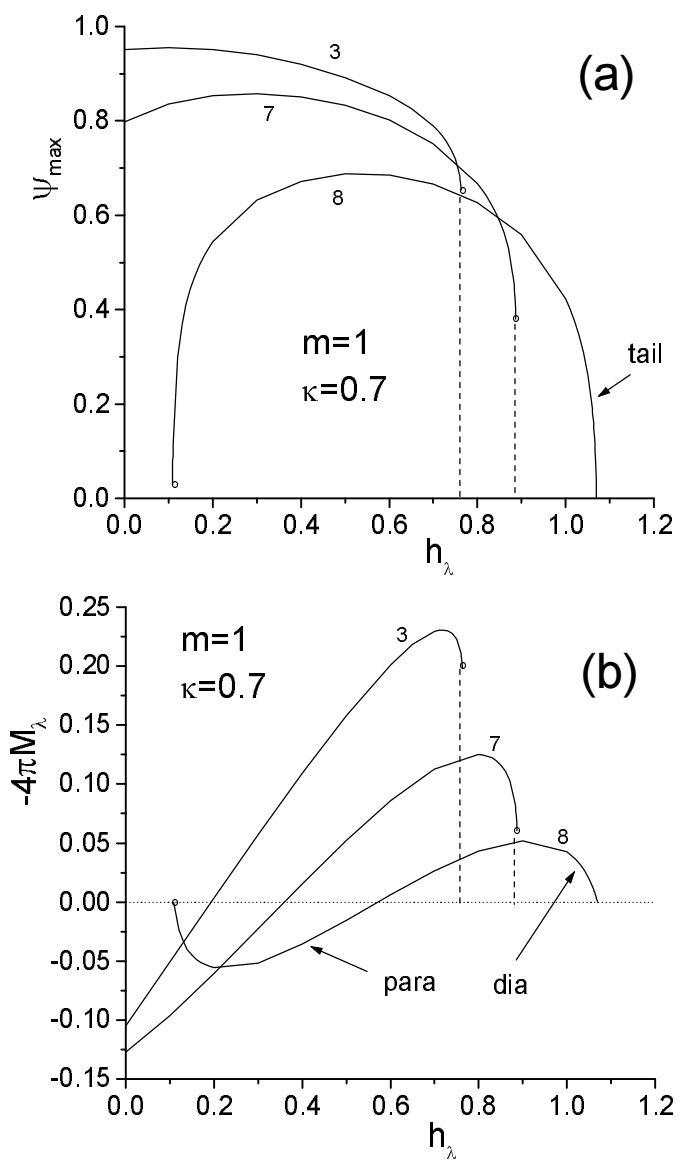


Fig. 4

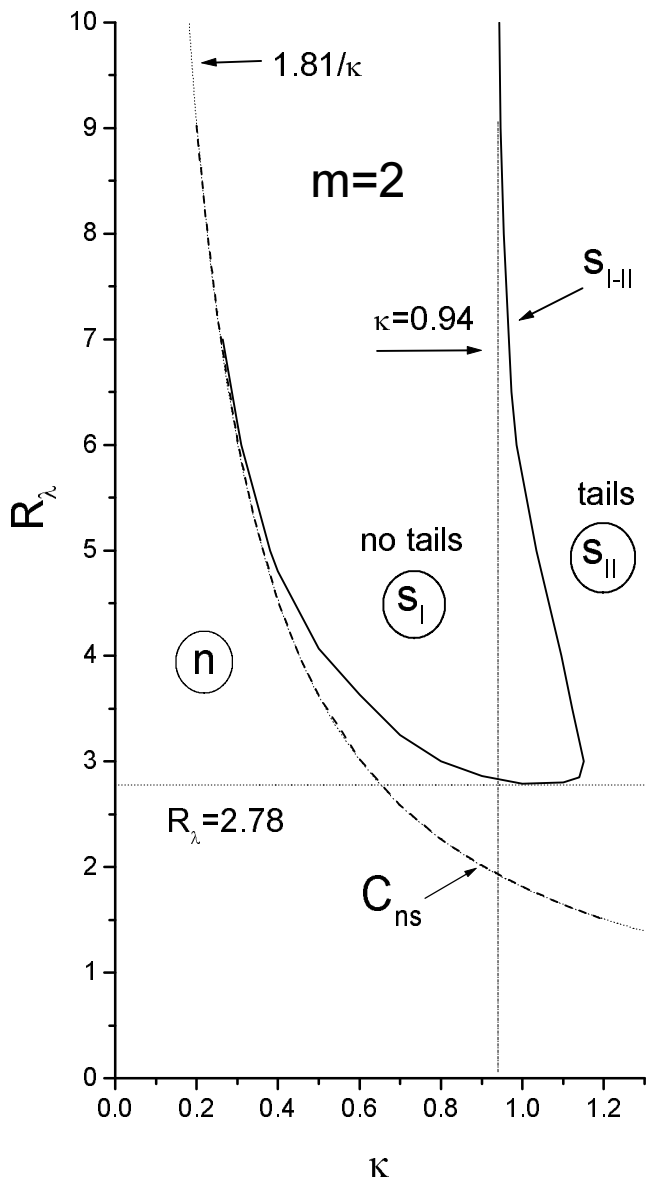


Fig. 5